

UCLA

UCLA Previously Published Works

Title

Minimizing table time in patients with claustrophobia using focused ferumoxylol-enhanced MR angiography (f-FEMRA): a feasibility study

Permalink

<https://escholarship.org/uc/item/1kb8g2cp>

Journal

British Journal of Radiology, 94(1125)

ISSN

0007-1285

Authors

Shahrouki, Puja
Nguyen, Kim-Lien
Moriarty, John M
et al.

Publication Date

2021-09-01

DOI

10.1259/bjr.20210430

Peer reviewed

Received:
05 April 2021Revised:
26 May 2021Accepted:
14 June 2021<https://doi.org/10.1259/bjr.20210430>

Cite this article as:

Shahrouki P, Nguyen K-L, Moriarty JM, Plotnik AN, Yoshida T, Finn JP. Minimizing table time in patients with claustrophobia using focused ferumoxytol-enhanced MR angiography (*f*-FEMRA): a feasibility study. *Br J Radiol* 2021; **94**: 20210430.

FULL PAPER

Minimizing table time in patients with claustrophobia using focused ferumoxytol-enhanced MR angiography (*f*-FEMRA): a feasibility study

PUJA SHAHROUKI, MD, KIM-LIEN NGUYEN, MD, JOHN M. MORIARTY, MD, ADAM N. PLOTNIK, MD, TAKEGAWA YOSHIDA, MD and J. PAUL FINN, MD

Department of Radiological Sciences, David Geffen School of Medicine at UCLA and VA Greater Los Angeles Healthcare System, Los Angeles, California, United States

Address correspondence to: J. Paul Finn
E-mail: pfinn@mednet.ucla.edu

Objectives: To assess the feasibility of a rapid, focused ferumoxytol-enhanced MR angiography (*f*-FEMRA) protocol in patients with claustrophobia.

Methods: In this retrospective study, 13 patients with claustrophobia expressed reluctance to undergo conventional MR angiography, but agreed to a trial of up to 10 min in the scanner bore and underwent *f*-FEMRA. Thirteen matched control patients who underwent gadolinium-enhanced MR angiography (GEMRA) were identified for comparison of diagnostic image quality. For *f*-FEMRA, the time from localizer image acquisition to completion of the angiographic acquisition was measured. Two radiologists independently scored images on both *f*-FEMRA and GEMRA for arterial and venous image quality, motion artefact and diagnostic confidence using a 5-point scale, five being best. Signal-to-noise ratio (SNR) and contrast-to-noise ratio (CNR) in the aorta and IVC were measured. The Wilcoxon rank-sum test, one-way ANOVA with Tukey correction and two-tailed *t* tests were utilized for statistical analyses.

Results: All scans were diagnostic and assessed with high confidence (scores ≥ 4). Average scan time for

f-FEMRA was 6.27 min (range 3.56 to 10.12 min), with no significant difference between *f*-FEMRA and GEMRA in diagnostic confidence (4.86 ± 0.24 vs 4.69 ± 0.25 , $p = 0.13$), arterial image quality (4.62 ± 0.57 vs 4.65 ± 0.49 , $p = 0.78$) and motion artefact score (4.58 ± 0.49 vs 4.58 ± 0.28 , $p > 0.99$). *f*-FEMRA scored significantly better for venous image quality than GEMRA (4.62 ± 0.42 vs 4.19 ± 0.56 , $p = 0.04$). CNR in the IVC was significantly higher for steady-state *f*-FEMRA than GEMRA regardless of the enhancement phase ($p < 0.05$).

Conclusions: Comprehensive vascular MR imaging of the thorax, abdomen and pelvis can be completed in as little as 5 min within the magnet bore using *f*-FEMRA, facilitating acceptance by patients with claustrophobia and streamlining workflow.

Advances in knowledge: A focused approach to vascular imaging with ferumoxytol can be performed in patients with claustrophobia, limiting time in the magnet bore to 10 min or less, while acquiring fully diagnostic images of the thorax, abdomen and pelvis.

BACKGROUND

Claustrophobia of some degree is found in a sizeable number of patients who are otherwise suitable candidates for contrast-enhanced MR angiography (CEMRA).¹ Conventional CEMRA protocols typically include pre-contrast imaging and multiphase postcontrast sequences, often with repeated contrast injections, such that examination times may exceed 30 min. Patients with claustrophobia, therefore, may be unwilling or unable to tolerate the examination. Several solutions have been proposed in large-scale studies to address these limitations including use of shorter, wider bore magnets,^{1,2} open low-field systems,³ sedation,^{4,5}

positioning,⁶ audio-visual aids^{1,7} and psychological interventions.⁸ To date, no consistent MR imaging approach has been developed that is easily implemented in clinical practice without increasing procedure times or compromising diagnostic image quality.

Whereas CEMRA has been widely used for more than two decades, recent advances in CT angiography (CTA) have highlighted the speed and simplicity of modern CTA when compared to CEMRA. Beyond challenges in workflow, the longer exam time associated with conventional MR techniques serves to discourage patients with even modest levels of claustrophobia. We have implemented a focused

ferumoxyl-enhanced MRA (*f*-FEMRA) protocol in patients with renal impairment, whereby targeted vascular imaging can be completed in only a few minutes within the magnet bore. The objectives of our study were 1) to assess the feasibility of *f*-FEMRA for rapid, extended field-of-view vascular imaging, 2) to evaluate whether *f*-FEMRA can be used to elicit compliance in patients with claustrophobia, and 3) to evaluate the diagnostic quality of the resulting images.

METHODS

This was a retrospective HIPAA-compliant and IRB-approved study where the study population provided written informed consent and the requirement for informed consent was waived in a control cohort of 13 age- and gender-matched patients who had previously undergone CEMRA with a gadolinium-based contrast agent (GBCA).

Patient population

We implemented an abbreviated, focused, ferumoxyl-enhanced MR angiography (*f*-FEMRA) protocol in 13 consecutive patients who were referred for FEMRA due to chronic kidney disease ($n = 12$) or hereditary haemorrhagic telangiectasia with anaemia ($n = 1$). All 13 patients were reluctant to undergo a conventional MR examination due to claustrophobia, but agreed to a trial of up to 10 min in the scanner bore.

An age- and gender-matched control cohort of 13 patients without chronic kidney disease was identified who underwent a successful CEMRA examination with a GBCA for identical indications as the study group. The imaging indications in both groups were central venous mapping ($n = 7$), aortic aneurysm ($n = 2$), central arterial occlusion/stenosis ($n = 2$), aortic stenosis ($n = 1$) or hereditary haemorrhagic telangiectasia ($n = 1$).

Image acquisition

For the *f*-FEMRA studies, no pre-contrast imaging was performed and ferumoxyl was infused outside the scanner bore at a rate of 0.5 mg/kg/min, to a total dose of 4 mg/kg. Heart rate, blood pressure and pulse oximetry were monitored continuously prior to, during and for up to 30 min following ferumoxyl infusion. Patients were positioned on the MRI scanner table and fitted with two body array coils, spanning the chest, abdomen and pelvis. They were then advanced into the scanner bore.

Automated scanner tuning and coil adjustment preceded localizer image acquisition. Patient-specific shimming was not performed and the default shim settings were used to minimize adjustment time. Following localizer sequences, breath-held, high-resolution 3-D FEMRA was carried out in one ($n = 1$) or two ($n = 12$) overlapping stations on a 3.0T MR system (Magnetom TIM Trio ($n = 8$), Magnetom Prisma Fit ($n = 3$) or Magnetom Skyra ($n = 2$); Siemens Medical Solutions, Malvern PA). Acquisition time for each station was 16–20 sec and typical voxel dimensions were 1x1.2 mm x 1.3 mm. The tune up time was less than 1 min and the scan time was measured from the beginning of localizer image acquisition to the end of the ultimate CEMRA. Partition (source) images from overlapping stations were composed inline into a set of extended field of view (*e*-FOV) images using

proprietary vendor software (Image Compose, Siemens), after the patients had left the MRI suite. Anatomic coverage for the FEMRA images was from the neck to the pelvis in 12 patients (*e*-FOV in two overlapping stations) or chest to abdomen in one patient (500 mm FOV in a single station).

The control cohort received gadobenate dimeglumine (MultiHance, Bracco, Princeton, NJ) (9–30 ml at 0.15 mmol/kg, $n = 13$) with a timed-bolus protocol on a 3.0T MR system (Magnetom TIM Trio ($n = 7$), Magnetom Prisma Fit ($n = 3$) or Magnetom Skyra ($n = 3$); Siemens Medical Solutions, Malvern PA) as previously described in detail.⁹ Anatomic coverage for the gadolinium-enhanced MRA (GEMRA) comprised chest to pelvis in two patients (*e*-FOV in two overlapping stations), chest to abdomen in eight patients (single station) and abdomen to pelvis in three patients (single station). Eleven patients in the control group were not claustrophobic and two patients who were claustrophobic were examined under general anesthesia. In the control group, no attempt was made to minimize examination time or streamline the acquisition protocol beyond institutional standard, since patients were chosen for their closely corresponding clinical indications to the study group.

Qualitative image analysis

Two board-certified senior radiologists (J.M.M. and A.N.P.) with more than 5 years of experience independently reviewed anonymized and randomized CEMRA images with no access to comparative imaging. Dynamic GEMRA images or steady-state *f*-FEMRA images were evaluated for each patient together with volume-rendered reformatted images and maximum intensity projection (MIP) reconstructions when available. The reviewers were aware of the imaging indication for each study. Studies were scored for confidence in diagnosis (1 = no confidence, 2 = low confidence, 3 = moderate confidence, 4 = high confidence, 5 = very high confidence). The images were scored for motion artefact (1 = severe motion artefact (non-diagnostic), 2 = moderate-severe motion artefact (diagnostic), 3 = moderate motion artefact (diagnostic), 4 = mild motion artefact (diagnostic), 5 = no motion artefact (diagnostic)). Finally, the reviewers indicated whether they would recommend additional imaging for complete assessment (yes or no). The reviewers further evaluated overall image quality with respect to arteries and veins on a 5-point scale (1 = Vessels not visualized or assessable due to non-diagnostic image quality, 2 = Vessels visualized, but size/patency cannot be assessed with confidence, 3 = Vessels defined but only size/patency are confidently assessable, 4 = Vessels well defined and segments evaluable for structural pathology with high confidence, 5 = Vessels have excellent definition with sharp borders and fine detail evaluable with high confidence).

Quantitative image analysis

The arterial and venous signal-to-noise ratio (SNR) and contrast-to-noise ratio (CNR) were measured by a single reviewer (T.Y.) on steady-state *f*-FEMRA images and on both arterial and venous phases of the GEMRA studies. Circular regions of interest were drawn in the inferior vena cava (IVC), abdominal aorta, adjacent liver and in non-anatomic background (air). The SNR was calculated by dividing the signal intensity of the IVC or aorta by the

Table 1. Patient Characteristics

	<i>f</i> -FEMRA (<i>n</i> = 13)	GEMRA (<i>n</i> = 13)	<i>P</i> value
Female sex ^a	6 (43)	6 (43)	
Age range (y)	11–84	10–85	
Mean age (y)	50.38 (25.19)	48.77 (25.39)	0.87
Pre-MRI creatinine (mg/dL)	3.90 (3.13)	0.73 (0.32)	<0.01
Chronic Kidney Disease	12 (92)	1 (8)	
Acute Kidney Injury	2 (15)	1 (8)	

Data are absolute values with percentages in parenthesis

^aData are mean with standard deviation in parenthesis *f*-FEMRA: focused feruxomylol-enhanced MR angiography, GEMRA: gadolinium-enhanced MR angiography (gadobenate dimeglumine)

standard deviation of the background (noise) and the CNR was calculated by dividing the difference in signal intensity between the IVC or aorta and adjacent tissue by the noise.

Clinical parameters

Retrospective analysis of the patient MRI and electronic medical record was carried out to document renal function before and after the CEMRA studies, total number and duration of acquisitions, need for additional imaging to the CEMRA studies and if additional steps were taken to minimize claustrophobia prior to the CEMRA study.

Statistical analysis

Continuous data are presented as means and standard deviations. Categorical and dichotomous data are presented as absolute values and percentages. Scan times are presented as means

and ranges. Data were tested for normality using the Shapiro–Wilk test. Intra group comparisons of SNR and CNR were made with Wilcoxon rank-sum test for paired samples. Intergroup comparisons of SNR and CNR were made with one-way ANOVA with Tukey correction. Comparisons between qualitative image scores and creatinine values were made with two-tailed *t* tests. Interobserver agreement was determined with Gwet's AC1 statistic due to higher interobserver agreement than κ value and constant rating,¹⁰ and was assessed as: 0.00–0.20, poor; 0.21–0.40, fair; 0.41–0.60, moderate; 0.61–0.80, good; 0.81–1.00, very good. Statistical analysis was performed by using SPSS software (version 25.0; SPSS, Chicago; Ill). Differences with *i*>p-values < 0.05 were considered statistically significant.

Table 2. Qualitative Image Scores of *f*-FEMRA and GEMRA

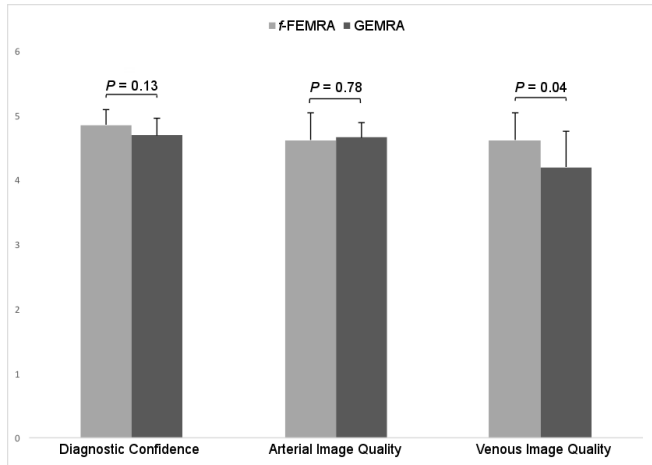
Qualitative Scoring Parameter	Average*	Observer 1*	Observer 2*	Interobserver agreement (AC1 value) ^a
Diagnostic confidence	0.49 (0.28, 0.71)
<i>f</i> -FEMRA	4.85 (0.24)	5.00 (0)	4.69 (0.48)	...
GEMRA	4.69 (0.25)	5.00 (0)	4.38 (0.51)	...
<i>P</i> value	0.125	N/Ab	0.125	...
Arterial Image Quality	0.26 (0.05, 0.47)
<i>f</i> -FEMRA	4.62 (0.42)	4.92 (0.28)	4.31 (0.48)	...
GEMRA	4.65 (0.24)	5.00 (0)	4.31 (0.63)	...
<i>P</i> value	0.78	0.33	>0.99	...
Venous Image Quality	0.28 (0.06, 0.50)
<i>f</i> -FEMRA	4.62 (0.42)	4.92 (0.28)	4.31 (0.63)	...
GEMRA	4.19 (0.56)	4.62 (0.65)	3.77 (0.73)	...
<i>P</i> value	0.04	0.13	0.05	...
Motion Artefact Score	0.30 (0.08, 0.51)
<i>f</i> -FEMRA	4.58 (0.49)	4.85 (0.38)	4.31 (0.75)	...
GEMRA	4.58 (0.28)	5.00 (0)	4.15 (0.55)	...
<i>P</i> value	>0.99	0.15	0.56	...

Data are mean with standard deviation in parenthesis.

^aData are absolute values with confidence intervals in parenthesis.

^b*t*-test could not be performed due to lack of variance.

Figure 1. Comparison of image quality score. Bars represent mean values, and error bars represent standard deviation. *f*-FEMRA: focused ferumoxytol-enhanced MR angiography, GEMRA: gadolinium-enhanced MR angiography (gadobenate dimeglumine).



RESULTS

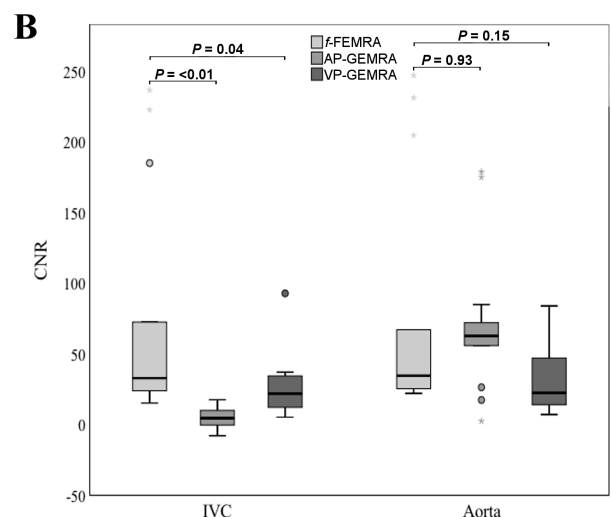
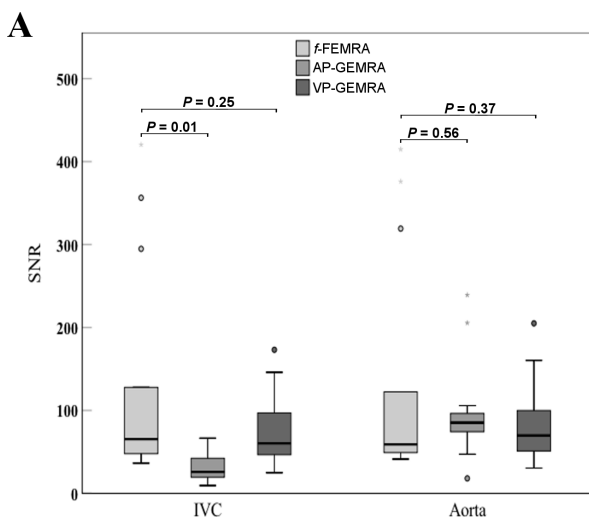
Of 443 consecutive FEMRA studies performed, thirteen patients (3%) were claustrophobic (age 11 to 84 years, 6 females) and expressed reluctance to undergo the procedure. Of these, 12 patients had renal failure (*n* = 12) and one had haemorrhagic hereditary telangiectasia. Patient characteristics for both *f*-FEMRA and GEMRA studies are outlined in Table 1. The average

f-FEMRA scan time was 6.27 min (range 3.56 to 10.12 min). The average GEMRA scan time for single station imaging (not determined in one patient with interspersed cardiac sequences) measured from the initial localizer image acquisition to the end of the ultimate MRA acquisition was 38.04 min (range 27.28 to 60.46 min). The *f*-FEMRA acquisition was repeated in 4 (31%) of 13 patients due to motion artefact on the first acquisition (Supplementary Material 1). The baseline creatinine was significantly higher in patients undergoing MRA with ferumoxytol than GBCAs ($3.90 \pm 3.13 \text{ mg dl}^{-1}$ vs $0.73 \pm 0.32 \text{ mg dl}^{-1}$, *p* < 0.01) and there was no significant difference in the pre- and post-MRI creatinine values for either group (*p* > 0.05).

Qualitative image analysis

Complete qualitative assessments are provided in Table 2. All scans were fully diagnostic, were assessed with high confidence (scores ≥ 4) and image quality did not differ significantly between *f*-FEMRA and GEMRA (4.86 ± 0.24 vs 4.69 ± 0.25 , *p* = 0.13). In all 26 (100%) studies, both reviewers indicated that additional imaging was not required to address the clinical questions. The arterial and venous anatomy was confidently evaluated (scores ≥ 3) in all patients. No significant difference in image quality was observed for arterial anatomy (4.62 ± 0.57 vs 4.65 ± 0.49 , *p* = 0.78), but significantly higher scores for venous anatomy on *f*-FEMRA compared to GEMRA studies was observed (4.62 ± 0.42 vs 4.19 ± 0.56 , *p* = 0.04 respectively). None of the final studies had motion artefact that impeded diagnostic assessment (scores ≥ 3) and there was no significant difference in artefact scores between *f*-FEMRA and GEMRA (4.58 ± 0.49 vs 4.58 ± 0.28 , *p* >

Figure 2. Box-whisker plot comparison of signal-to-noise ratio (SNR; A) and contrast-to-noise ratio (CNR; B) between focused ferumoxytol-enhanced MR angiography (*f*-FEMRA), arterial phase and venous phase gadolinium-enhanced MR angiography (GEMRA). Outliers were defined as 1.5 interquartile range (circles) and extreme values were defined as 3 interquartile range (stars). IVC: inferior vena cava.



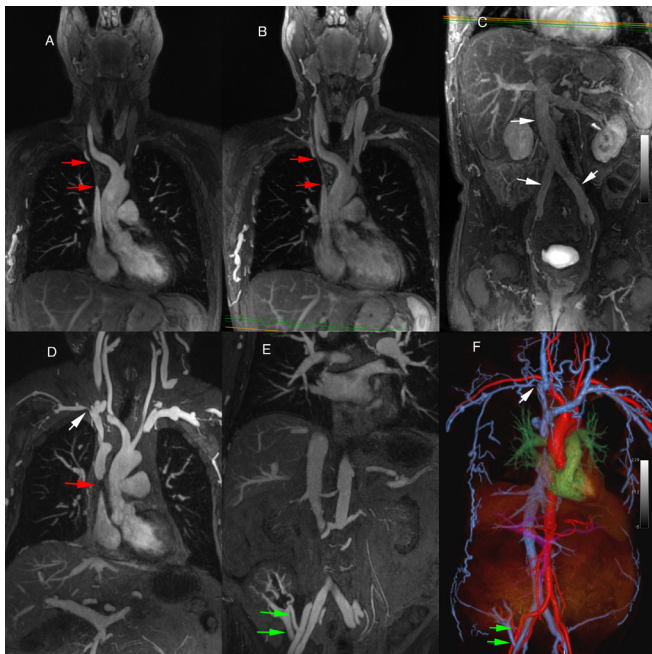
	f-FEMRA	GEMRA		
		Arterial phase (AP)	Venous phase (VP)	P-value (AP vs VP GEMRA)
IVC	65.4 (46.1 – 211.3)	25.9 (16.4 – 43.0)	60.3 (46.0 – 105.6)	<0.01
Aorta	59.0 (48.9 – 220.8)	85.2 (63.5 – 101.1)	69.8 (48.9 – 112.0)	0.08
P-value (IVC vs aorta)	0.09	<0.01	0.18	

Data are median with interquartile range (IQR) in parenthesis.

	f-FEMRA	GEMRA		
		Arterial phase (AP)	Venous phase (VP)	P-value (AP vs VP GEMRA)
IVC	32.8 (22.8 – 128.8)	4.5 (-3.3 – 11.2)	21.9 (11.6 – 34.6)	<0.01
Aorta	34.5 (24.5 – 135.9)	62.7 (41.1 – 78.5)	22.5 (13.2 – 59.0)	<0.01
P-value (IVC vs aorta)	0.09	<0.01	0.18	

Data are median with interquartile range (IQR) in parenthesis.

Figure 3. GEMRA at 3.0T (a,b,c) in a 59-year-old male with SVC occlusion (red arrows in arterial phase MIP, a and venous phase MIP, (b). The IVC and common iliac veins are widely patent (white arrows in venous phase MIP, (c). Separate injections of gadodiamide were used for upper and lower stations and total examination time for multiphase GEMRA was more than 40 min. Two station 3.0T *f*-FEMRA (d,e,f) in a 61-year-old male shows SVC occlusion (red arrow in 3a, MIP), right subclavian stenosis (white arrow in 3d and 3f) and widely patent transplant renal artery and vein (green arrows 3e and 3f). 3f is a colour rendered e-FOV image derived from a combined two-station acquisition. The total examination time for the *f*-FEMRA was 7 min and four seconds.



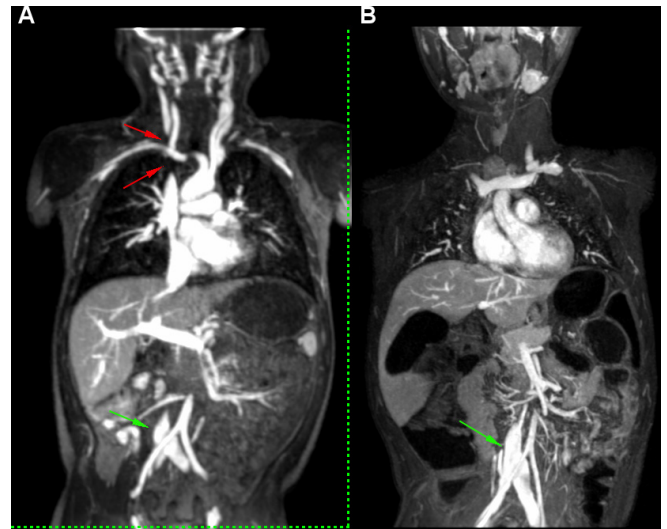
0.99). **Figure 1** summarizes the comparison of the image quality scores between *f*-FEMRA and GEMRA.

The interobserver agreement was moderate for diagnostic confidence (AC1 = 0.49, 95% CI: 0.28, 0.71) and fair for arterial image quality (AC1 = 0.26, 95% CI: 0.05, 0.47), venous image quality (AC1 = 0.28, 95% CI: 0.06, 0.50) and motion artefact score (AC1 = 0.30, 95% CI: 0.08, 0.51).

Quantitative image analysis

Comparison of the SNR and CNR for steady-state *f*-FEMRA and GEMRA is presented in **Figure 2**. The SNR and CNR of the IVC show a significant increase from the arterial to the venous phase of GEMRA ($p < 0.01$ for both) signifying time-dependent venous enhancement. The SNR of the aorta on GEMRA shows a trend toward decreased signal intensity from the arterial to the venous phase ($p = 0.08$) and the CNR of the aorta shows a significant decrease ($p < 0.01$) over the same time interval, signifying time-dependent arterial enhancement. The *f*-FEMRA in steady-state had noninferior SNR and CNR of the aorta compared to both GEMRA in the arterial ($p = 0.56$ and 0.93 respectively) and venous ($p = 0.37$ and 0.15 respectively) phases. The CNR of the IVC for *f*-FEMRA in steady-state was significantly higher than

Figure 4. Two pediatric patients with suspected central venous occlusion. Single-station 3.0T *f*-FEMRA (a) in an 11-year-old male without anesthesia shows right innominate vein occlusion (red arrows). The FEMRA acquisition was repeated four times due to motion artifacts before the final satisfactory set was acquired, such that the total examination time was 10 min and 12 sec. Single-station 3.0T GEMRA (b) carried out in a 10-year-old female under full anesthesia (b) showed widely patent veins, with uniformly high signal in the IVC in both studies (green arrows).



both arterial and venous phases of GEMRA ($p < 0.01$ and $p = 0.04$ respectively).

On *f*-FEMRA images, there was no significant difference in SNR or CNR of the aorta and IVC ($p = 0.09$ for both), suggesting uniform distribution of contrast within the arterial and venous vascular beds.

Figures 3–6 exemplify image quality and contrast enhancement achieved with ferumoxytol- and gadolinium-enhanced MRAs.

Figure 5. Five sequential *f*-FEMRA acquisitions were carried out in the 11-year-old male from **Figure 3**. Three representative *f*-FEMRA images (a-c) show progressively better vessel border definition (red arrows) due to increasing compliance with breath hold instructions. There are ghost artifacts due to motion (green arrows) in a and b) that are absent in the final acquisition.

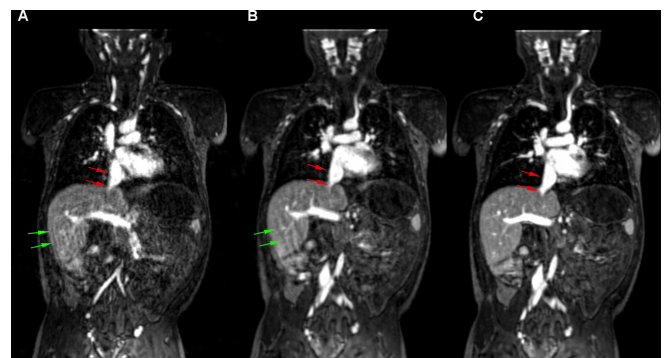
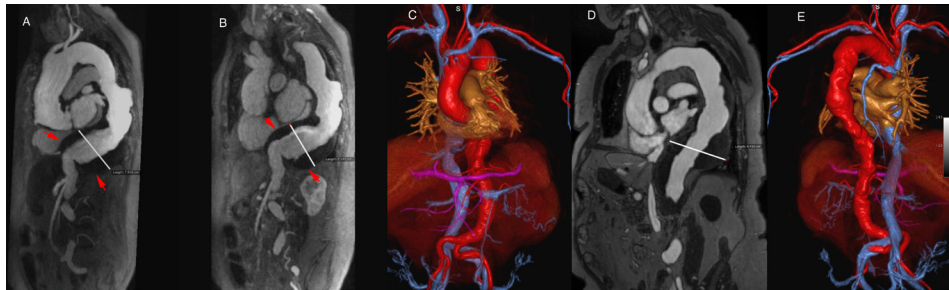


Figure 6. Single station, two-phase GEMRA in an 85 year old female with an 8cm fusiform aneurysm of the distal thoracic aorta (cursor on MIP of arterial phase, 6a and venous phase, 6b), associated with mural thrombus (red arrows in a,b). Examination time was 24min and 15sec. *f*-FEMRA (6c,d,e) in an 84 year-old female with 9.5cm fusiform thoraco-abdominal aortic aneurysm with mural thrombus (cursor on MIP image, 6d). Color volume rendering (6c, (e) highlights the perfused lumen throughout the aorta and iliac arteries. Examination time was 7min and 45sec.



Clinical outcomes

Supplemental imaging beyond CEMRA was carried out in two patients with *f*-FEMRA and two patients with GEMRA at the request of the referring physician. In one patient, ultrasound was requested following *f*-FEMRA in a patient with suspected central venous occlusion after a radiology trainee's initial read (Figure 5). Uncertainty was resolved by the faculty radiologist on service and corresponded fully with the ultrasound findings. In a second patient, non-contrast CTA followed *f*-FEMRA to determine the extent of aortic calcification in a patient with suspected pseudo renal artery stenosis (Figure 7). One patient with GEMRA required complementary imaging with contrast-enhanced CTA in the setting of pre-procedural planning for an aortic aneurysm. Right heart catheterization complemented the second patient's GEMRA with suspected severe aortic stenosis to help in pre-operative planning. Two of the patients undergoing GBCA-MRA were claustrophobic and required anesthesia. None of the patients undergoing FEMRA required anesthesia.

DISCUSSION

The results of our study show that, using focused acquisition during the steady state distribution of ferumoxytol, comprehensive vascular imaging of the thorax, abdomen and pelvis can be completed in as little as 4 min in the scanner bore. The stable vascular signal due to ferumoxytol allowed for extended field of view imaging in multiple stations and, even with repeated acquisitions, the longest period within the scanner bore was 10 min.

Compared to GEMRA, *f*-FEMRA provided non-inferior vascular image quality, confidence in diagnosis and motion artefact score. Moreover, the venous image quality was higher in *f*-FEMRA than GEMRA, consistent with the higher measured CNR in the IVC on *f*-FEMRA compared to venous phase GEMRA. *e*-FOV reconstruction by combining multistation acquisitions is trivial with ferumoxytol, whereas it is often challenging with GEMRA due to dynamic changes in contrast concentration.¹¹ *e*-FOV imaging with *f*-FEMRA allowed for confident pre-surgical planning in patients with aortic disease whereas GEMRA required additional imaging in two patients, suggesting that FEMRA may be superior to GEMRA for certain

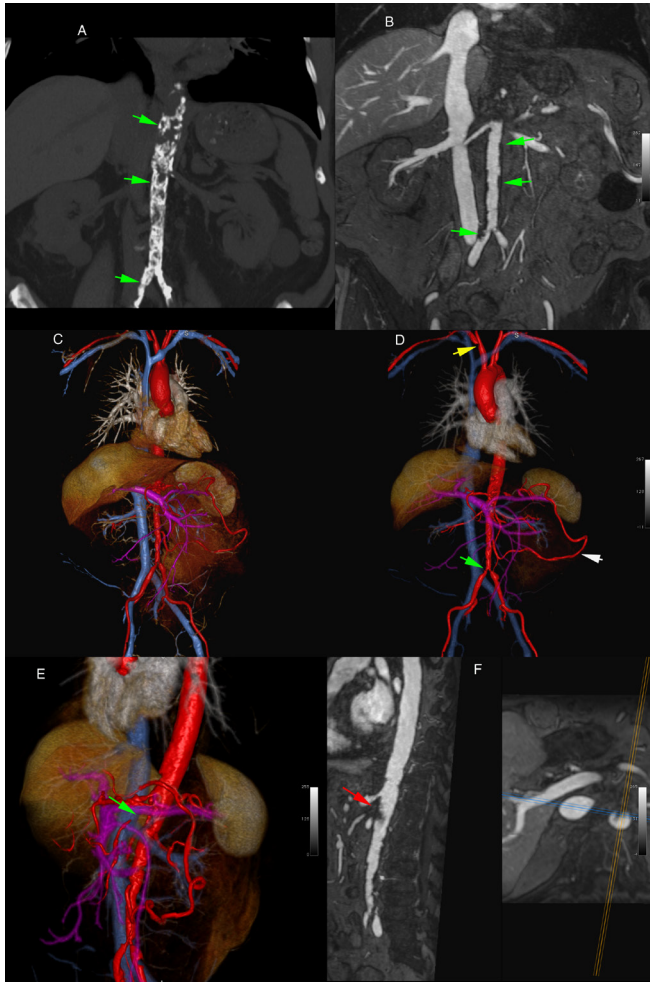
applications. The value of FEMRA for pre-operative planning of TAVR has previously been demonstrated in patients with severe aortic stenosis.^{12,13}

The implications of our findings for imaging patients who are claustrophobic, anxious, distressed or in discomfort are significant. FEMRA in the steady state eliminates the requirement for first pass imaging and bolus timing, without undermining diagnostic quality in the chest, abdomen and pelvis, where differentiation of arterial and venous anatomy is straightforward.¹⁴⁻¹⁷ For imaging the lower extremity or intracranial vessels, arterial-venous separation can be more problematic and the optimal approach to using ferumoxytol for these territories remains to be determined.^{18,19}

The prevalence of claustrophobia in our FEMRA cohort was found to be 3%, which is on the same order of magnitude as previously reported.¹ The overall negative impact of lengthy MRI scans may be underestimated however, as the population analyzed for our quoted prevalence does not account for patients who may have refused completely to undergo conventional MRI and were not offered *f*-FEMRA. Further, the spectrum of anxiety related to MR imaging was not specifically addressed, which may or may not affect image quality but does affect the patient experience. Although not required in our study patients, the steady-state distribution of ferumoxytol would allow patients to take breaks from being inside the scanner bore and go back in for short periods to complete a study. It is known that the perception of not being able to exit the MR scanner aggravates claustrophobia,²⁰ suggesting that patients may comply with a staggered approach of short periods rather than a prolonged, uninterrupted series of acquisitions, where anxiety can build. With GBCAs, staggered image acquisition is not practical without repeated contrast injection. The stable MR signal during steady-state distribution of ferumoxytol ensures consistent vascular enhancement. Among current commercially available MRI contrast agents, these are unique attributes of ferumoxytol.

Several limitations of our study need to be addressed. The *f*-FEMRA protocol was carried out in a small cohort of

Figure 7. 79 year-old male patient with renal impairment and abdominal bruit. MIP of non-contrast CT (7a) and *f*-FEMRA (7b) show severe aortic calcification (green arrows). Note clear visualization of the perfused aortic lumen in 7b. e-FOV *f*-FEMRA with color 3D volume rendering (7c,d) confirm extensive distal aortic disease (green arrow in 7d), stenosis of the right subclavian artery (yellow arrow in 7d) and an enlarged inferior mesenteric artery forming an Arc of Riolan (white arrow in 7d). Occlusion of the proximal superior mesenteric artery is highlighted in 7e,f (arrows). Examination time for *f*-FEMRA was 6 min and 46 sec.



claustrophobic patients with relative contraindications to gadolinium or iodinated contrast. Our study, however, was designed to address the feasibility and practicality of a truncated imaging protocol as applied to patients with claustrophobia, and our findings provide strong preliminary evidence that our approach is likely to be generalizable. Larger patient studies will be required to establish the more general validity of our hypothesis.

Another limitation is that only gadobenate dimeglumine was used as a GBCA in the control group, reflecting local institutional practice. However, multiple studies have shown the noninferior properties of gadobenate dimeglumine in thoracic, abdominal and pelvic MRA when compared to other

extracellular GBCAs^{21,22} and thus it serves as a reasonable representative of currently available GBCAs. The GBCA gadofosveset (previously marketed as Ablavar, Lantheus Medical, Billerica, MA) had a longer intravascular half-life than the purely extracellular agents, but it is no longer marketed in the US.²³ Ferumoxytol, therefore, is the only remaining intravascular MRI contrast agent clinically available for off-label diagnostic use and the spectrum of clinical applications specific to a true intravascular agent is now focused squarely on its domain.

In clinical therapy trials, ferumoxytol was administered as a rapid (30 mg/sec) bolus, delivering 500 mg over 17 sec. At this dose and rate, the reported serious adverse event rate was 0.2%.²⁴ Ferumoxytol was approved for bolus therapeutic use from 2009 to 2015. In March, 2015, based on postmarketing reports, the FDA issued a black box warning about potential hypersensitivity reactions and withdrew approval for bolus administration.²⁵ Updated FDA guidelines now require slow intravenous infusion, similar to the other intravenous iron therapy agents. Following satisfactory supplemental safety trials by the manufacturer (AMAG, MA) in January, 2018, the FDA expanded the approval for ferumoxytol therapy to include patients without renal impairment who are intolerant of oral iron or in whom oral iron is ineffective.²⁶

We found no adverse events in our study and multiple single-center and a single multi center study have found a very low incidence of severe adverse events with the diagnostic use of ferumoxytol.^{27,28}

As confirmed in our study, the vascular signal during the steady state distribution of ferumoxytol is independent of both the speed of injection and the time between injection and image acquisition, in keeping with recent reports.²⁹ Therefore, injection protocols can be fully compatible with updated FDA safety guidelines that recommend slow infusion, without compromising image quality.²⁵

CONCLUSION

In conclusion, we implemented a focused approach to vascular imaging with ferumoxytol in patients with claustrophobia, limiting time in the magnet bore to 10 min or less, while acquiring fully diagnostic images of the thorax, abdomen and pelvis. The implications for workflow efficiency and clinical impact for patients needing MR angiography are significant.

AUTHORS' CONTRIBUTIONS

PS participated in the design, acquisition of data, analysis and interpretation of data, and drafted the manuscript. KLN participated in the design and manuscript preparation. JMM scored the studies, acquired the images and revised the manuscript. AP scored the studies and revised the manuscript. TY participated in acquisition of data and revised the manuscript. JPF conceived the study, participated in the design, acquired the images, and revised the manuscript. All authors read and approved the final manuscript.

COMPETING INTERESTS

JPF has served on the Speakers Bureau for Bayer Pharma and on an advisory panel for Bracco Diagnostics within the past year. The other authors declare that they have no competing interests.

FUNDING

Not applicable.

CONSENT FOR PUBLICATION

Written informed consent for publication of individual data and accompanying images was obtained from all 13 study partici-

pants in the experimental group, and waived in 13 study participants of the control cohort. The consent form is available for review by the Editor-in-Chief if requested.

ETHICS APPROVAL AND CONSENT TO PARTICIPATE

All thirteen patients in the experimental group provided written informed consent and the requirement for informed consent was waived in a control cohort of 13 age- and gender-matched patients. The study was approved by the local Institutional Review Board and conformed to the Health Portability and Insurance Accountability Act.

REFERENCES

- Dewey M, Schink T, Dewey CF. Claustrophobia during magnetic resonance imaging: cohort study in over 55,000 patients. *J Magn Reson Imaging* 2007; **26**: 1322–7. doi: <https://doi.org/10.1002/jmri.21147>
- Hunt CH, Wood CP, Lane JI, Bolster BD, Bernstein MA, Witte RJ, Wide WRJ. Wide, short bore magnetic resonance at 1.5 T: reducing the failure rate in claustrophobic patients. *Clin Neuroradiol* 2011; **21**: 141–4. doi: <https://doi.org/10.1007/s00062-011-0075-4>
- Calabrese M, Brizzi D, Carbonaro L, Chiaramondia M, Kirchin MA, Sardanelli F. Contrast-Enhanced breast MR imaging of claustrophobic or oversized patients using an open low-field magnet. *Radiol Med* 2009; **114**: 267–85. doi: <https://doi.org/10.1007/s11547-008-0358-2>
- von Knobelsdorff-Brenkenhoff F, Bublak A, El-Mahmoud S, Wassmuth R, Opitz C, Schulz-Menger J. Single-Centre survey of the application of cardiovascular magnetic resonance in clinical routine. *Eur Heart J Cardiovasc Imaging* 2013; **14**: 62–8. doi: <https://doi.org/10.1093/ehjci/jes125>
- Francis JM, Pennell DJ. Treatment of claustrophobia for cardiovascular magnetic resonance: use and effectiveness of mild sedation. *J Cardiovasc Magn Reson* 2000; **2**: 139–41. doi: <https://doi.org/10.3109/10976640009148683>
- Eshed I, Althoff CE, Hamm B, Hermann K-GA. Claustrophobia and premature termination of magnetic resonance imaging examinations. *J Magn Reson Imaging* 2007; **26**: 401–4. doi: <https://doi.org/10.1002/jmri.21012>
- Lemaire C, Moran GR, Swan H. Impact of audio/visual systems on pediatric sedation in magnetic resonance imaging. *J Magn Reson Imaging* 2009; **30**: 649–55. doi: <https://doi.org/10.1002/jmri.21870>
- Lang EV, Ward C, Laser E. Effect of team training on patients' ability to complete MRI examinations. *Acad Radiol* 2010; **17**: 18–23. doi: <https://doi.org/10.1016/j.acra.2009.07.002>
- Nguyen K-L, Khan SN, Moriarty JM, Mohajer K, Renella P, Satou G, et al. High-Field MR imaging in pediatric congenital heart disease: initial results. *Pediatr Radiol* 2015; **45**: 42–54. doi: <https://doi.org/10.1007/s00247-014-3093-y>
- Gwet KL. Computing inter-rater reliability and its variance in the presence of high agreement. *Br J Math Stat Psychol* 2008; **61**(Pt 1): 29–48. doi: <https://doi.org/10.1348/000711006X126600>
- Kramer H, Quick HH, Tombach B, Schoenberg SO, Barkhausen J. Whole-Body MRA. *Eur Radiol* 2008; **18**: 1925–36. doi: <https://doi.org/10.1007/s00330-007-0817-5>
- Nguyen K-L, Moriarty JM, Plotnik AN, Aksoy O, Yoshida T, Shemin RJ, et al. Ferumoxytol-enhanced Mr angiography for vascular access mapping before transcatheter aortic valve replacement in patients with renal impairment: a step toward patient-specific care. *Radiology* 2018; **286**: 326–37. doi: <https://doi.org/10.1148/radiol.2017162899>
- Kallianos K, Henry TS, Yeghiazarians Y, Zimmet J, Shunk KA, Tseng EE, et al. Ferumoxytol MRA for transcatheter aortic valve replacement planning with renal insufficiency. *Int J Cardiol* 2017; **231**: 255–7. doi: <https://doi.org/10.1016/j.ijcard.2016.12.147>
- Anzai Y, Prince MR, Chenevert TL, Maki JH, Londy F, London M, et al. Mr angiography with an ultrasound superparamagnetic iron oxide blood pool agent. *J Magn Reson Imaging* 1997; **7**: 209–14. doi: <https://doi.org/10.1002/jmri.1880070132>
- Bashir MR, Jaffe TA, Brennan TV, Patel UD, Ellis MJ. Renal transplant imaging using magnetic resonance angiography with a nonnephrotoxic contrast agent. *Transplantation* 2013; **96**: 91–6. doi: <https://doi.org/10.1097/TP.0b013e318295464c>
- Bashir MR, Mody R, Neville A, Javan R, Seaman D, Kim CY, et al. Retrospective assessment of the utility of an iron-based agent for contrast-enhanced magnetic resonance venography in patients with endstage renal diseases. *J Magn Reson Imaging* 2014; **40**: 113–8. doi: <https://doi.org/10.1002/jmri.24330>
- Hope MD, Hope TA, Zhu C, Faraji F, Haraldsson H, Ordovas KG, et al. Vascular imaging with Ferumoxytol as a contrast agent. *AJR Am J Roentgenol* 2015; **205**: W366–73. doi: <https://doi.org/10.2214/AJR.15.14534>
- Lehrman ED, Plotnik AN, Hope T, Saloner D. Ferumoxytol-enhanced MRI in the peripheral vasculature. *Clin Radiol* 2019; **74**: 37–50. doi: <https://doi.org/10.1016/j.crad.2018.02.021>
- Walker JP, Nosova E, Sigovan M, Rapp J, Grenon MS, Owens CD, et al. Ferumoxytol-enhanced magnetic resonance angiography is a feasible method for the clinical evaluation of lower extremity arterial disease. *Ann Vasc Surg* 2015; **29**: 63–8. doi: <https://doi.org/10.1016/j.avsg.2014.09.003>
- Thorpe S, Salkovskis PM, Dittner A. Claustrophobia in MRI: the role of cognitions. *Magn Reson Imaging* 2008; **26**: 1081–8. doi: <https://doi.org/10.1016/j.mri.2008.01.022>
- Fink C, Puderbach M, Ley S, Risse F, Kuder TA, Bock M, et al. Intraindividual comparison of 1.0 M gadobutrol and 0.5 M gadopentetate dimeglumine for time-resolved contrast-enhanced three-dimensional magnetic resonance

- angiography of the upper torso. *J Magn Reson Imaging* 2005; **22**: 286–90. doi: <https://doi.org/10.1002/jmri.20381>
22. Herborn CU, Lauenstein TC, Ruehm SG, Bosk S, Debatin JF, Goyen M. Intraindividual comparison of gadopentetate dimeglumine, gadobenate dimeglumine, and gadobutrol for pelvic 3D magnetic resonance angiography. *Invest Radiol* 2003; **38**: 27–33. doi: <https://doi.org/10.1097/00004424-200301000-00004>
23. Finn JP, Nguyen K-L, Hu P. Ferumoxytol vs. gadolinium agents for contrast-enhanced MRI: thoughts on evolving indications, risks, and benefits. *J Magn Reson Imaging* 2017; **46**: 919–23. doi: <https://doi.org/10.1002/jmri.25580>
24. Lu M, Cohen MH, Rieves D, Pazdur R. Fda report: Ferumoxytol for intravenous iron therapy in adult patients with chronic kidney disease. *Am J Hematol* 2010; **85**: NA–9. doi: <https://doi.org/10.1002/ajh.21656>
25. Food and Drug AdministrationFDA Drug Safety Communication: FDA strengthens warnings and changes prescribing instructions to decrease the risk of serious allergic reactions with anemia drug Feraheme (ferumoxytol). 2015. Available from: <https://www.fda.gov/Drugs/DrugSafety/ucm440138.htm>.
26. Food and Drug AdministrationFERAHEME® (ferumoxytol injection), for intravenous use. 2018. Available from: https://www.accessdata.fda.gov/drugsatfda_docs/label/2018/022180s009lbl.pdf.
27. Ahmad F, Treanor L, McGrath TA, Walker D, McInnes MDF, Schieda N. Safety of off-label use of Ferumoxytol as a contrast agent for MRI: a systematic review and meta-analysis of adverse events. *J Magn Reson Imaging* 2021; **53**: 840–58. doi: <https://doi.org/10.1002/jmri.27405>
28. Nguyen K-L, Yoshida T, Kathuria-Prakash N, Zaki IH, Varallyay CG, Semple SI, et al. Multicenter safety and practice for off-label diagnostic use of Ferumoxytol in MRI. *Radiology* 2019; **293**: 554–64. doi: <https://doi.org/10.1148/radiol.2019190477>
29. Shahrouki P, Moriarty JM, Khan SN, Bista B, Kee ST, DeRubertis BG, et al. High resolution, 3-dimensional Ferumoxytol-enhanced cardiovascular magnetic resonance venography in central venous occlusion. *J Cardiovasc Magn Reson* 2019; **21**: 17. doi: <https://doi.org/10.1186/s12968-019-0528-5>